

## **Corrosion behaviour of reduced activation ferritic/martensitic steel (RAFMS) and P91 (9Cr- 1Mo) steel in static lead-lithium eutectic**

**Shahrukh Shamim, Danish Raza and Joseph Damor**

*Department of Material Science and Metallurgical Engineering, National Institute of Technology, Bhopal, Madhya Pradesh, India*

---

### **ABSTRACT**

*Reduced Activation Ferritic/Martensitic Steel (RAFMS) is used as a structural material in fusion energy systems. It is presently under development by several laboratories for the Indian Test Blanket Module for ITER. This paper presents the outcome of the compatibility of RAFM and P91 (9Cr-1Mo) Steel (as-received and cold worked) with static lead-17% lithium for 355 hours at two different temperatures viz. 823 K and 923 K. Suitable corrosion rates for RAFMS and P91 in Pb-17% Li are established. The effect of corrosion on the structural and morphological properties along with the possible mechanism of corrosion is studied. After 355 h of operation, samples of RAFMS and P91 both as-received and cold worked were analysed with the help of weight change measurements and Scanning Electron Microscope coupled with Energy Dispersive Spectroscopy (SEM-EDS). The results showed preferential dissolution of metallic species like Fe, Cr and Mn from P91 as-received samples leading to weight loss. At lower temperature both as-received and cold worked samples of RAFMS gained weight due to oxidation, predominantly at the boundary region. Dissolution and deposition rates are found to be increasing with temperature in both P91 and RAFM steel specimens.*

**Keywords:** Corrosion, Reduced Activation Ferritic/Martensitic Steel, P91, Static Lead Lithium eutectic, SEM-EDS

---

### **INTRODUCTION**

One of the key challenges in the nuclear fusion reactor concerns the compatibility of materials with the coolant. With a primary aim of in-house tritium breeding, Lead Lithium eutectic (Pb-17% Li) is proposed as the coolant, breeder and neutron multiplier. It provides effective tritium breeding and safer, relative to molten lithium, due to its less reactivity with air and water [1]. However, a serious problem arising from the use of Pb-17% Li is the corrosion of the containment material and its deleterious effect on the mechanical properties. Pb-17% Li has been found to be more corrosive than pure lithium and the rate of corrosion is affected by various factors like temperature, flow velocity, etc. [1,2]. It was found that austenitic steels have a poor resistance to Pb- 17% Li because of the high solubility of nickel [3,4]. Presently, Reduced-activation ferritic/martensitic steels are considered as promising candidates for fusion reactor components. Its development has been promoted in order to simplify special containment of highly radioactive structures of fusion reactor which has a better corrosion resistance than other conventional Cr-Mo steels.

The reduced activation composition adopted for fusion structural materials has involved the substitution of alloying elements like Mo, Ni and Nb present in the commercial martensitic steels by other elements which exhibit faster decay of induced radioactivity, such as Ta, W and V [5]. With this objective a new reduced activation ferritic/martensitic steel, named RAFMS has been developed. Its chemical composition has been designed and optimized to obtain good corrosion characteristics comparable to conventional Cr-Mo steels. The main purpose of this paper is to evaluate the effect of temperature and cold working on the corrosion behaviour of RAFMS in static lead lithium eutectic and to compare it with the behaviour of P91 Steel, a material studied as a candidate structural

material for fusion reactors [6]. Modified 9Cr- 1Mo is primarily designed for developing creep resistant alloys for fast breeder power reactor programs [7-9].

## MATERIALS AND METHODS

The experimental setup used in the present work is shown in Figure 1. The material used for this study is reduced activation ferritic/martensitic steel (RAFM) and P91 steel (9Cr- 1Mo) in as-received and cold worked conditions and having dimensions shown in Table 1. The chemical composition of RAFM steel used is (wt.%): 0.11% C, 8.8% Cr, 0.5% Mn, 0.22% V, 1.0% W, 0.007% Ta, 0.003% N, <0.005% Ti, <0.001% Nb, <0.002% Mo, <0.005% Ni, <0.002% S, balance Fe, and the composition of P91 steel is (wt.%): 0.006% C, 9.12% Cr, 1.09% Mo, 0.39% Mn, 0.14% Ni, 0.25% V, 0.14% Nb, balance Fe. The entire setup was fabricated from a combination of two SS316L pipes having internal diameter 25mm and 4mm wall thickness. Kenthal heaters covered with aluminium ceramic beads along with K type thermocouples were wrapped on the pipe as indicated in Figure 1. All the heaters are connected through PID controllers. A thin 200 mm long Molybdenum strip is used to place the samples axially inside the tubes. Pb-17% Li chunks were placed in the SS316L tubes and a positive cover gas pressure of argon was maintained over the entire setup. The temperature of tube A was raised and maintained at 823 K (550 °C) whereas tube B was maintained at a temperature of 923 K (650 °C).

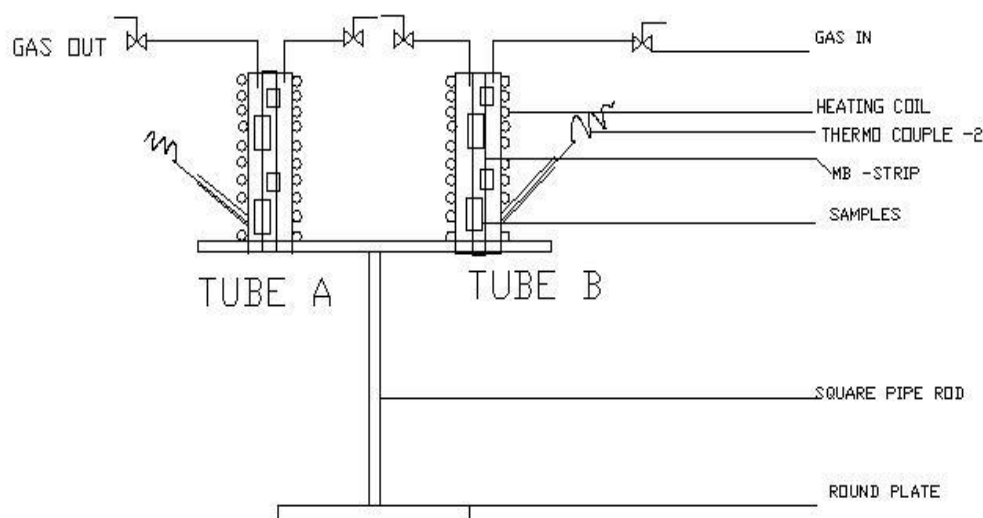


Figure 1: Schematic drawing of the corrosion testing setup

Table 1a: Dimensions of RAFM and P91 steel

Samples	Tube A: RAFMS		Tube B: RAFMS	
	As-Received	Cold Worked	As-Received	Cold Worked
<b>Dimensions (mm)</b>				
<b>Length</b>	20	21	20	21
<b>Breadth</b>	12	14	12	15
<b>Thickness</b>	3	2	3	2
<b>Weight (gm.)</b>	5.620	4.659	5.565	5.234
Samples	Tube A: P91Steel		Tube B: P91 Steel	
	As-Received	Cold Worked	As-Received	Cold Worked
<b>Dimensions (mm)</b>				
<b>Length</b>	12	13	13	12
<b>Breadth</b>	9.5	9.7	9.7	9.4
<b>Thickness</b>	2	1	1.7	1.7
<b>Weight (gm.)</b>	1.434	1.002	1.570	0.982

After 355 h of operation, RAFM and P91 steel samples were taken out from SS316L tubes under argon atmosphere. The samples were cleaned off the adhering solidified Pb-17% Li by repeatedly exposing it to a mixture of acetic acid, acetone and hydrogen peroxide mixed in the ratio 1:1:1. The cleaned samples were used for further characterization.

The corrosion rate of RAFMS and P91 steel samples in static Pb-17% Li was quantified as a function of time using weight loss measurements. Microstructural and compositional analysis was carried out by Scanning Electron Microscopy coupled with Energy Dispersive Spectroscopy (SEM-EDS). For characterization, samples were etched in Picral (picric acid and ethanol).

**RESULTS AND DISCUSSION**

Weight loss data for RAFMS and P91 steel samples, in as-received and cold worked conditions, at both the temperature is shown in Table 2. As observed from the table, dissolution rate in P91 steel (as-received condition) at 923 K is higher than the rate at 823 K and hence rate of dissolution is increasing with temperature. On the other hand, Table 3 shows the increase in weight of RAFM and P91 steel samples (as-received and cold worked condition).

**Table 2: Dissolution rate of RAFMS and P91 steel samples at 823 K and 923 K**

Temperature (K)	Samples	Initial weight (gm.)	Final weight (gm.)	loss (gm.)	Dissolution rate ( $\mu\text{g}/\text{cm}^2 \text{ h}$ )
823 K	P91(as-received)	1.434	1.433	0.001	0.08
	RAFMS (cold worked)	5.234	5.226	0.008	2.91
923 K	P91(as-received)	1.570	1.55	0.02	17.15

**Table 3: Deposition rate of RAFMS and P91 steel samples at 823 K and 923 K**

Temperature (K)	Samples	Initial weight (gm.)	Final weight (gm.)	Gain (gm.)	Deposition rate ( $\mu\text{g}/\text{cm}^2 \text{ h}$ )
823 K	RAFMS(as-received)	5.620	5.636	0.016	6.70
	RAFMS(cold worked)	4.659	4.662	0.003	1.16
	P91(cold worked)	1.002	1.004	0.002	1.89
923 K	RAFMS(as-received)	5.565	5.592	0.027	11.31
	P91(cold worked)	0.982	0.990	0.008	7.55

As indicated in Table 3, deposition rate for RAFM steel (as-received) at 923 K is higher than the rate at lower temperature. Deposition rate in cold worked P91 steel samples shows increment with temperature. The RAFM and P91 steel samples were subjected to microstructural and compositional analysis after cleaning of the adherent layer of Pb-17% Li. Figure 2a&b shows the microstructure of RAFM steel (as-received) after exposure to Pb-17% Li at 823 K and 923 K respectively. Figure 2a clearly shows the deposition of lead on the surface of the sample. Composition of these samples was obtained from EDS (Fig 3a&b) and is reported in Table 4, both at boundary and matrix region. The boundary region of the sample indicated the presence of 24.69% oxygen whereas at matrix, small amount of oxygen is present. Iron and chromium content is found to be increasing from boundary to the matrix region, indicating the deposition of metallic species resulting in weight gain. On examining the microstructure of P91 steel samples (Figure 4a), whitish layer of lead-lithium is deposited on the surface of the steel when exposed at 823 K. At higher temperature, microstructure shows dissolution of metallic species from both boundary and matrix region (Figure 4b).

Compositional analysis of P91 steel specimen is shown in Table 5 as obtained from EDS Fig 5a&b. Results indicate almost same amount of oxygen content at both boundary as well as at matrix region. Iron and chromium content is depleted from the as-received P91 steel specimen at 923 K, which accounts for the weight loss. On the contrary, cold worked sample shows deposition of metallic species like Iron, Chromium and Molybdenum on the surface.

**Table 4: Composition of RAFM steel sample**

Elements	Weight%	
	At Boundary	At Matrix
Oxygen	24.69	4.31
Chromium	6.57	9.55
Iron	64.77	85.04
Tungsten	1.66	0.91
Lead	0.77	0.20
Tantalum	1.46	-
Manganese	0.08	-

**Table 5: Composition of P91 steel sample**

Elements	Weight%	
	At Boundary	At Matrix
Oxygen	22.74	23.62
Chromium	6.07	7.29
Iron	69.74	67.75
Manganese	0.38	0.42
Molybdenum	0.64	0.93
Lead	0.44	-

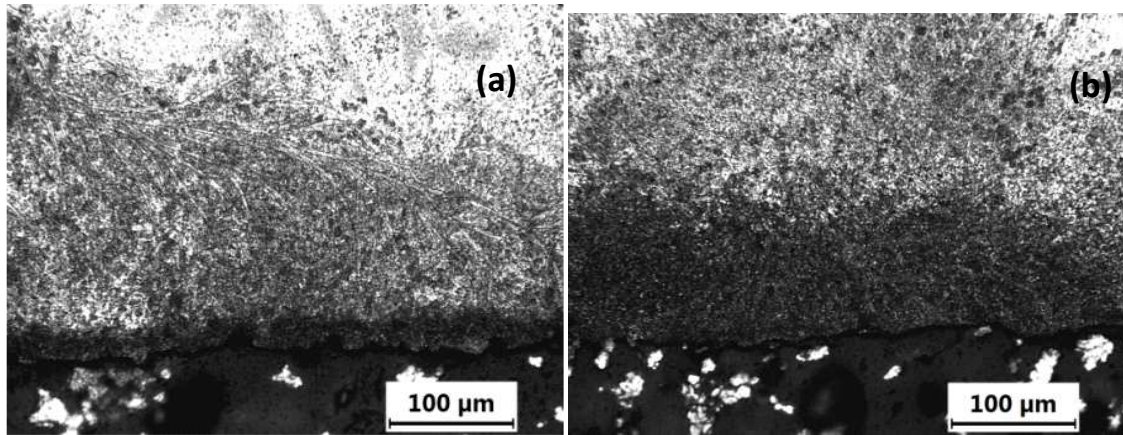


Figure 2: (a) Microstructure of RAFM steel after exposure in Pb-17% Li at 823 K, (b) RAFM steel sample at 923 K indicating the deposition of metallic species.

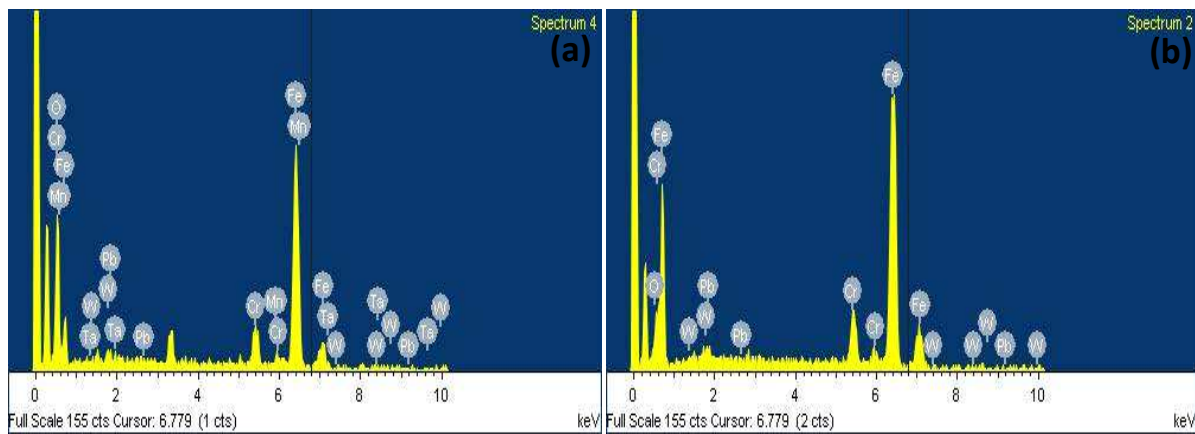


Figure 3: Compositional analysis of RAFM steel after exposure (a) at the boundary region, (b) at the matrix region

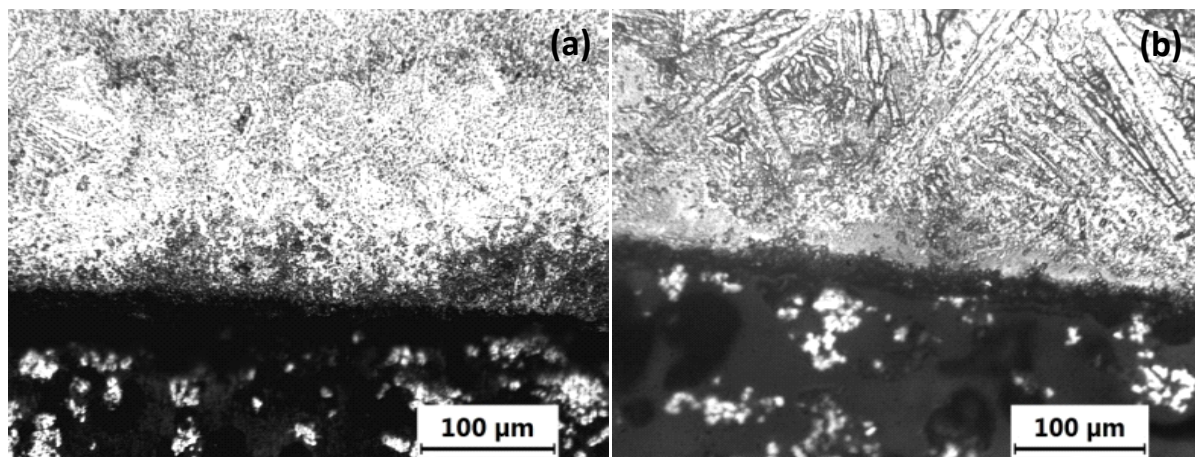


Figure 4: (a) Microstructure of P91 specimen after exposure showing deposition of Lead, (b) P91 steel specimen indicating weight loss due to depletion of Iron and Chromium

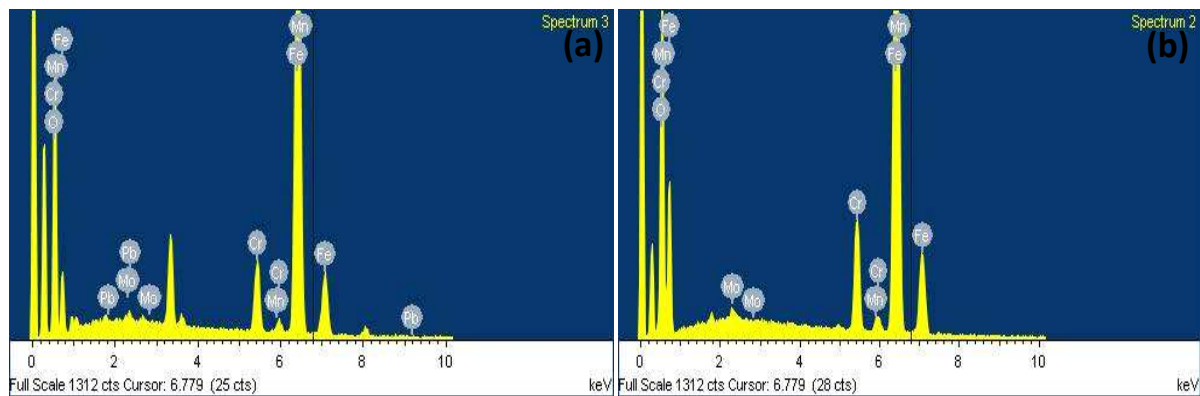


Figure 5: Compositional analysis of P91 steel after exposure (a) at the boundary region, (b) at the matrix region

### CONCLUSION

RAFM and P91 steel samples were exposed to static lead-17% lithium eutectic at 823 K and 923 K. After 355 h, the dissolution rate of P91 steel (As-Received) at 823 K and 923 K is  $0.08 \mu\text{g}/\text{cm}^2\text{h}$  and  $17.15 \mu\text{g}/\text{cm}^2\text{h}$  respectively. Test results revealed that corrosion of P91 specimen initiates by dissolution of the oxide layer present on its surface. Non-uniform dissolution of P91 creates a non-uniformly exposed surface from which corrosion proceeds mainly by the dissolution of major alloying elements like Cr and Fe into Pb–17Li. On the contrary, dissolution rate of RAFM steel (cold worked) at 923 K is  $2.91 \mu\text{g}/\text{cm}^2\text{h}$ . At 823 K, deposition rate of RAFM steel both cold worked and as-received samples are found to be 1.16 and  $6.70 \mu\text{g}/\text{cm}^2\text{h}$  respectively, due to Iron, chromium and molybdenum deposition at the boundary region. RAFM steel samples at 923 K shows high deposition rate of  $11.31 \mu\text{g}/\text{cm}^2\text{h}$  whereas deposition rate in P91 steel samples, cold worked, at 823 K and 923 K is  $1.89 \mu\text{g}/\text{cm}^2\text{h}$  and  $7.55 \mu\text{g}/\text{cm}^2\text{h}$  respectively.

### REFERENCES

- [1] Atanov A, Chepovski A, Gromov V, Kalinin G, Markov V, Rybin V, et al. *Fusion Eng Des*, **1991**;14:213–8.
- [2] Malang S, Mattas R.. *Fusion Eng Des*, **1995**; 27: 399–406.
- [3] Tortorelli PF. *J Nucl Mater*, **1992**;191–194:965–9.
- [4] Simon N, Terlain A, Flament T. *Corros Sci*, **2001**;43:1041–52.
- [5] A. Kohyama, A. Hishinuma, D.S. Gelles, et al., *J. Nucl. Mater.*, 233–237 (1996) 138–147.
- [6] Poulami Chakraborty, Pankaj Kumar Pradhan, Ram Krishen Fotedar, Nagaiyar Krishnamurthy. *J. Mater Res Technol*, **2013**;2(3):206–212.
- [7] Saroja S, Dasgupta A, Divakar R, Raju S, Mohandas E, Vijayalakshmi M, et al. *J Nucl Mater*, **2011**;409:131–9.
- [8] Hsu C-Y, Lechtenberg TA. *J Nucl Mater*, **1986**;141–143:1107–12.
- [9] Zeman A, Debarberis L, Kořčík J, Slugeň V, Keilová E. *J Nucl Mater*, **2007**;362:259–67.